the first (bending) and second (torsion) structural modes, with the bending mode going unstable. The initial physical model predicts that it is the second mode that goes unstable. However, when this model is tuned using experimental data available at 50, 60, and 65 psf, the correct flutter mechanism is then predicted. Although the damping ratio of the first mode dips sharply at 65 psf and seems to indicate flutter to occur at 70 psf, the proposed approach still predicts the correct flutter boundary. This shows the interest of relying both on experimental data and also physically significant models.

V. Conclusion

A simple method for flight flutter clearance is presented. This method uses both an analytical model of the flexible dynamics of the wing (or aircraft) and wind-tunnel (or in-flight) experimental data. The advantage of this method in comparison to traditional flight flutter clearance methods is its ability to produce reliable flutter boundary estimates using the experimental data obtained in flight conditions still far away from flutter. The proposed method is validated on a wind-tunnel experiment. The results show that the method can considerably improve the flutter boundary estimates compared with predictions provided by an analytical model alone. An operational implementation of the proposed flutter prediction procedure would require significantly more work, including the automation of many of the aforementioned steps.

Appendix: Physical Models

The mass matrix M is normalized to be the identity. The stiffness matrix K and damping matrix D are 3 by 3 and diagonal, with the following diagonal elements:

$$K = \text{diag}[277.237 \quad 8266.0 \quad 13250.0]$$
$$C = \text{diag}[0.402940 \quad 2.909361 \quad 2.923759] \tag{A1}$$

The lag poles are $\beta_1 = 0.187999$ and $\beta_2 = 4.096000$. The normalizing constant is $b = 6.75$ in. and density $\rho = 1.1478.10^{-7}\text{lb} \cdot \text{s}^2/\text{in.}^4$. The initial aerodynamic matrices estimates are also 3 by 3 and are given by

$$A_0 = \begin{bmatrix} -467.39 & -836.00 & 144.10 \\ 3397.00 & 5760.00 & -758.00 \\ 1467.00 & 4004.00 & 531.80 \end{bmatrix}$$

$$A_1 = \begin{bmatrix} -6391.50 & -5789.52 & 5959.07 \\ 3948.12 & -4559.45 & -844.78 \\ 10946.81 & 8498.99 & -15977.31 \end{bmatrix}$$

$$A_2 = \begin{bmatrix} -2805.96 & -763.30 & 1554.89 \\ -1266.69 & -3005.82 & 1978.34 \\ 1261.52 & 1217.91 & -5060.74 \end{bmatrix} \tag{A2}$$

$$A_3 = \begin{bmatrix} -90.01 & -81.70 & 66.36 \\ -477.65 & -722.58 & 281.67 \\ 25.19 & -10.05 & -37.16 \end{bmatrix}$$

$$A_4 = \begin{bmatrix} 13887.78 & 8605.01 & -20329.47 \\ 10067.41 & 10532.87 & -18437.83 \\ -20113.66 & -13183.07 & 32900.46 \end{bmatrix}$$

Acknowledgments

This research was funded by NASA Dryden Flight Research Center, M. Brenner serving as the Technical Monitor. The authors would like to thank J. Dugundji, E. Crawley, and C. Lin for their help.

References

[1]Kehoe, M. W., "A Historical Overview of Flight Flutter Testing," *Proceedings of the 80th AGARD Structures and Materials Panel, AGARD-CP-566*, Rotterdam, The Netherlands, 1995, pp. 1.1–1.15.

[2]Cooper, J., "Parameter Estimation Methods for Flight Flutter Testing," *Proceedings of the 80th AGARD Structures and Materials Panel, AGARD-CP-566*, Rotterdam, The Netherlands, 1995, pp. 10.1–10.12.

[3]Lin, C., "Towards Optimal Strain Actuated Aeroelastic Control," Ph.D. Thesis, Dept. of Aeronautics and Astronautics, Massachusetts Inst. of Technology, Cambridge, MA, Feb. 1996.

[4]Gupta, K., Brenner, M., and Voelker, L., "Development of an Integrated Aeroservoelastic Analysis Program and Correlation with Test Data," NASA TP-3120, May 1991.

[5]Hassig, H., "An Approximate True Damping Solution of the Flutter Equation by Determinant Iteration," *Journal of Aircraft*, Vol. 8, No. 11, 1971, pp. 885–889.

[6]Nissim, E., and Gilyard, G. B., "Method for Experimental Determination of Flutter Speed by Parameter Identification," *30th Structures, Structural Dynamics, and Materials Conference*, AIAA, Washington, DC, April 1989, pp. 1427–1441 (AIAA Paper 89-1324, 1989).

[7]Brenner, M., and Lind, R., "Robust Flutter Margins of an F/A-18 Aircraft from Aeroelastic Flight Data," *Journal of Guidance, Control, and Dynamics*, Vol. 20, No. 3, 1997, pp. 597–604.

[8]Feron, E., Brenner, M., Paduano, J., and Turevskiy, A., "Time-Frequency Analysis for the Transfer Function Estimation and Application to Flutter Clearance," *Journal of Guidance, Control, and Dynamics*, Vol. 21, No. 3, 1998, pp. 375–382.

[9]Karpel, M., and Strul, E., "Minimum-State Unsteady Aerodynamic Approximations with Flexible Constraints," *Journal of Aircraft*, Vol. 33, No. 6, 1996, pp. 1190–1196.

[10]Balas, G., Doyle, J., Glover, K., Packard, A., and Smith, R., "μ-Analysis and Synthesis Toolbox," MathWorks, Natick, MA, 1994.

[11]Gill, P. E., Murray, W., and Wright, M., *Practical Optimization*, Academic, London, 1994, pp. 115–125.

[12]Reich, G., VanSchoor, M., Lin, C., and Crawley, E., "An Active Aeroelastic Wing Model for Vibration and Flutter Suppression," *36th Structures, Structural Dynamics, and Materials Conference*, AIAA, Washington, DC, April 1995, pp. 314–324 (AIAA Paper 95-1193, 1995).

Discrete-Time Optimal Guidance

R. Gitizadeh* and I. Yaesh†
Israeli Military Industries,
47100 Ramat-Hasharon, Israel
and
J. Z. Ben-Asher‡
Wales, Ltd., 52521 Ramat-Gan, Israel

I. Introduction

MODERN guidance techniques are based mainly on optimal control theory and on differential games.[1,2] Most problems formulated with these methods are solved for continuous-time systems, whereas discrete-time systems are treated numerically.[3] However, most of the applications require discrete-time realizations. In the present work, the most popular guidance problems will be formulated and analytically solved for discrete-time systems. To this end we will use the linear model of a planar pursuit–evasion conflict, assuming ideal pursuer and evader systems.

We consider an evader maneuvering with a constant acceleration and derive discrete-time versions of the proportional navigation (PN) and augmented proportional navigation (APN) guidance laws. These guidance laws turn out to have the same structure as

Received Feb. 25, 1998; revision received Aug. 2, 1998; accepted for publication Aug. 2, 1998.

*Research Engineer, Department of Control and Simulation, IMI-ASD, P.O. Box 1044-77.

†Head, Department of Control and Simulation, IMI-ASD, P.O. Box 1044-77.

‡System Engineer, Hayetsira 29; currently Associate Professor, Department of Aerospace Engineering, Technion—Israel Institute of Technology, 32000 Haifa, Israel. Senior Member AIAA.

the continuous-time PN and APN laws but with different navigation constants. We also derive the discrete-time versions of the optimal rendezvous (OR) laws of Ref. 1.

II. Problem Formulation

The zero-order-hold discrete-time model of an ideal pursuer–evader system can be shown to have the following form[1,2]:

$$X(t_{k+1}) = \begin{bmatrix} 1 & h \\ 0 & 1 \end{bmatrix} X(t_k) + \begin{bmatrix} h^2/2 \\ h \end{bmatrix} (u(t_k) - w(t_k)) \tag{1}$$

where x_1 and x_2, the components of X, are the relative displacement and velocity, respectively, and h is the sampling time. The driving inputs u and w are the corresponding normal accelerations of the pursuer and the evader.

We introduce the following cost-function:

$$J = \frac{1}{2} b x_1^2(t_N) + \frac{1}{2} c x_2^2(t_N) + \frac{h}{2} \sum_{i=0}^{N-1} \left[u^2(t_i) \right] \tag{2}$$

which is the discrete-time version of the continuous-time cost function

$$J = \frac{1}{2} b x_1^2(t_f) + \frac{1}{2} c x_2^2(t_f) + \frac{1}{2} \int_{t_0}^{t_f} u^2(t)\, \mathrm{d}t \tag{3}$$

where

$$\frac{t_f - t_0}{h} = N \tag{4}$$

In Eq. (2) $b > 0$ is the penalty imposed by the miss-distance requirement, i.e., the relative separation at the final time. Typically, we let $c = 0$; however, we may also consider cases where the pursuer's objective is to minimize the terminal lateral velocity ($c > 0$) or even cases where the pursuer's objective is to maximize this velocity ($c < 0$). This objective depends heavily on the particular conflict for which the problem is formulated.[4]

Naturally, for perfect intercepts ($x_1(t_N) = 0$) we will require that

$$b \to \infty \tag{5}$$

and for perfect rendezvous,[1] where $x_1(t_N) = 0$ and $x_2(t_N) = 0$, we will require that

$$b \to \infty, \qquad c \to \infty \tag{6}$$

We further assume that the target applies constant evasive maneuvers, but the maneuvers are exactly known.

III. General Solution

We let $w(t_k) = w_0$ and rewrite Eq. (1) as

$$X(t_{k+1}) = \begin{bmatrix} 1 & h \\ 0 & 1 \end{bmatrix} X(t_k) + \begin{bmatrix} h^2/2 \\ h \end{bmatrix} (u(t_k) - w_0) \tag{7}$$

where $X(t_0)$ is given. We want to find the control vector sequence $u(t_k)$, $k = 0, 1, \ldots, N-1$ that minimizes the quadratic form (2). Based on optimal control theory[1] the optimal control may be expressed in feedback form (see Ref. 5 for details) as follows:

$$u = -(g_1 x_1 + g_2 x_2 + g_3 w_0) \tag{8}$$

where

$$g_1 = \frac{6b\left(hct_{\mathrm{go}} + h - ct_{\mathrm{go}}^2 - 2t_{\mathrm{go}}\right)}{-12 - 4bt_{\mathrm{go}}^3 + t_{\mathrm{go}} bh^2 - bct_{\mathrm{go}}^4 - 12ct_{\mathrm{go}} + cbh^2 t_{\mathrm{go}}^2} \tag{9}$$

$$g_2 = \frac{3t_{\mathrm{go}}^2 hbc + 6t_{\mathrm{go}} bh - 4cbt_{\mathrm{go}}^3 - 12c + ct_{\mathrm{go}} bh^2 - 12t_{\mathrm{go}}^2 b}{-12 - 4bt_{\mathrm{go}}^3 + t_{\mathrm{go}} bh^2 - bct_{\mathrm{go}}^4 - 12ct_{\mathrm{go}} + cbh^2 t_{\mathrm{go}}^2} \tag{10}$$

$$g_3 = \frac{-t_{\mathrm{go}}\left(-12c + 3bht_{\mathrm{go}} - cbt_{\mathrm{go}}^3 + ct_{\mathrm{go}} bh^2 - 6t_{\mathrm{go}}^2 b\right)}{-12 - 4bt_{\mathrm{go}}^3 + t_{\mathrm{go}} bh^2 - bct_{\mathrm{go}}^4 - 12ct_{\mathrm{go}} + cbh^2 t_{\mathrm{go}}^2} \tag{11}$$

and where $t_{\mathrm{go}} = (N - i)h$.

The formulas for g_1, g_2, and g_3 are quite intricate; hence, we look at two important special cases.

A. Case Without Velocity Weighting: Discrete Augmented Proportional Navigation (DAPN)

For this case $c = 0$ and $b \to \infty$, and from Eqs. (9–11), we get

$$g_1 = \frac{6}{t_{\mathrm{go}}(h + 2t_{\mathrm{go}})} \tag{12}$$

$$g_2 = \frac{6}{h + 2t_{\mathrm{go}}} \tag{13}$$

$$g_3 = \frac{-3t_{\mathrm{go}}}{h + 2t_{\mathrm{go}}} \tag{14}$$

The line-of-sight rate is given by[2]

$$\dot{\lambda} = \frac{x_1 + x_2 t_{\mathrm{go}}}{V_C t_{\mathrm{go}}^2} \tag{15}$$

where V_C is the closing velocity. Using the last relations we find that

$$u = -N'[V_C \dot{\lambda} - (w_0/2)] \tag{16}$$

where

$$N' = \frac{6t_{\mathrm{go}}}{h + 2t_{\mathrm{go}}} \tag{17}$$

Therefore, the APN law for a discrete-time system is the guidance law of Eq. (16) when N' is given in Eq. (17).

Taking $h \to 0$, we get

$$N' = \left. \frac{6t_{\mathrm{go}}}{h + 2t_{\mathrm{go}}} \right|_{h=0} = 3 \tag{18}$$

which is the well-known APN constant for the continuous-time case. Using the definition of $t_{\mathrm{go}} = (N - i)h$ we obtain

$$N' = \frac{6(N - i)}{1 + 2(N - i)} \tag{19}$$

For $(N - i) \gg 1$, we obtain $N' = 3$, and N' is smaller as we approach the target. When $(N - i) = 1$, we obtain $N' = 2$. Note also that when $w_0 = 0$ the discrete-time version of the PN is obtained.

B. Perfect Intercept with Terminal Velocity Weighting: Discrete Augmented Optimal Rendezvous (DAOR)

The perfect rendezvous is obtained from Eqs. (9–11) by letting

$$b \to \infty, \qquad c \to \infty \tag{20}$$

We obtain the following feedback gains:

$$g_1 = \frac{6}{t_{\mathrm{go}}(h + t_{\mathrm{go}})} \tag{21}$$

$$g_2 = \frac{h + 4t_{\mathrm{go}}}{t_{\mathrm{go}}(h + t_{\mathrm{go}})} \tag{22}$$

$$g_3 = -1 \tag{23}$$

Using the relation $\lambda = y/(V_c t_{\mathrm{go}})$ we find that

$$u = -V_c(\overline{g_1}\lambda + \overline{g_2}\dot{\lambda}) + w \tag{24}$$

where

$$\overline{g_1} = \frac{2t_{\mathrm{go}} - h}{t_{\mathrm{go}}(t_{\mathrm{go}} + h)}, \qquad \overline{g_2} = \frac{4t_{\mathrm{go}} + h}{t_{\mathrm{go}} + h} \tag{25}$$

Taking $h \to 0$, we get

$$\overline{g_1} = 2/t_{\mathrm{go}}, \qquad \overline{g_2} = 4 \tag{26}$$

which is the well-known augmented optimal rendezvous (AOR) for the continuous-time case.[1] The preceding control law has the structure of PN and an additional feedback from the line-of-sight angle. Thus, given the line-of-sight angle and its rate, perfect rendezvous can be easily mechanized.

IV. Numerical Simulations

A. Perfect Intercept

In this section the effects of three guidance laws for the perfect intercepts case will be analyzed. In this example the closing velocity is 300 m/s and $t_f = 3$ s. We assume a low-rate sampling time of 0.1 s. For example, this may be the case when global positioning system data are used for homing purposes. Three different guidance laws are compared.

1. APN

We use a sampled version of the PN guidance law with $N' = 3$. The guidance laws will be designed using the control $\boldsymbol{u}$ sampled with $h = 0.1$ s.

2. DAPN

This is the guidance law of Eq. (16) when N' is given by Eq. (17). Similar to APN, guidance laws will be designed using the control $\boldsymbol{u}$ sampled with $h = 0.1$ s.

3. Augmented Proportional Navigation for Continuous-Time System (APNC)

This guidance law is exactly like APN, except the control signal is not sampled (for this case we take an integration step of $h = 0.0001$). In all cases, the target will be allowed to perform an evasive maneuver involving a switch in the acceleration polarity at time-to-go of 0.3 s, namely,

$$w(t) = \begin{cases} 10g & t < t_f - 0.3 \\ -10g & t \geq t_f - 0.3 \end{cases}$$

Figures 1 and 2 show the performance of all three guidance laws in the presence of this evasive maneuver. In Fig. 1, the relative separation is in meters, whereas Fig. 2 shows the missile acceleration in g's. The solid line represents the DAPN, the dashed line the APN, and the dotted line the APNC. The miss distances are all small (zero for APNC, 0.0255 m for DAPN, and 0.1048 m for APN), but the required acceleration for DAPN guidance is significantly lower than for APN and even lower than for APNC.

Moreover, note that the DAPN shows a striking similarity to APNC (Fig. 1). To explain the implication of these results we first need to remind the reader of a well known and important observation that was made in Ref. 2 (page 153) about the navigation constant N' in minimum effort continuous-time guidance, where the pursuer is characterized by a single time lag. It was observed there that the special dependence of N', which is 3 far from the target and becomes unbounded near hit, effectively cancels the effect of the pursuer dynamics. This was seen in Ref. 2 by comparing the trajectories of proportional navigation with $N' = 3$, for ideal pursuer and single-lag pursuer cases, with the trajectory of the minimum effort guidance law with the single-lag pursuer. Surprisingly, the trajectory of minimum effort law with a single-lag pursuer and the trajectory of the $N' = 3$ law (which is the minimum effort law for the ideal pursuer) are identical. This also seems to the case in discrete-time guidance. The optimal discrete-time law effectively cancels the sampling effect.

We finally note that for this example reducing h to 0.03 s narrows the differences between the competing guidance laws to an insignificant level.

B. Perfect Rendezvous

In this section the three guidance laws for the perfect rendezvous case will be analyzed. In this example, the closing velocity is 300 m/s and t_f is 0.5 s. As before the guidance laws will be evaluated using the control $\boldsymbol{u}$ sampled at 10 Hz. Three different guidance laws are compared.

1) AOR is the guidance law of Eqs. (24) and (25) with $h = 0$.

2) DAOR is the guidance law of Eqs. (24) and (25) with the actual h.

3) The augmented optimal rendezvous for continuous-time system (AORC) guidance law is exactly like AOR, except the control signal is not sampled. The target will be allowed to maneuver similar to Sec. IV.A, and we assume $x_2(t_0) = 26.2$ m/s, which corresponds to a 5-deg heading, and $x_1(t_0) = 20$ m.

Figure 3 presents the relative lateral velocity for the three cases. Here, again, the optimal discrete-time law effectively cancels the sampling effort. The terminal velocity values were 0.02 m/s for AORC, 0.18 m/s for DAOR, and 2.45 m/s for AOR. Moreover, AOR lead to larger cost than the DAPN and APNC.

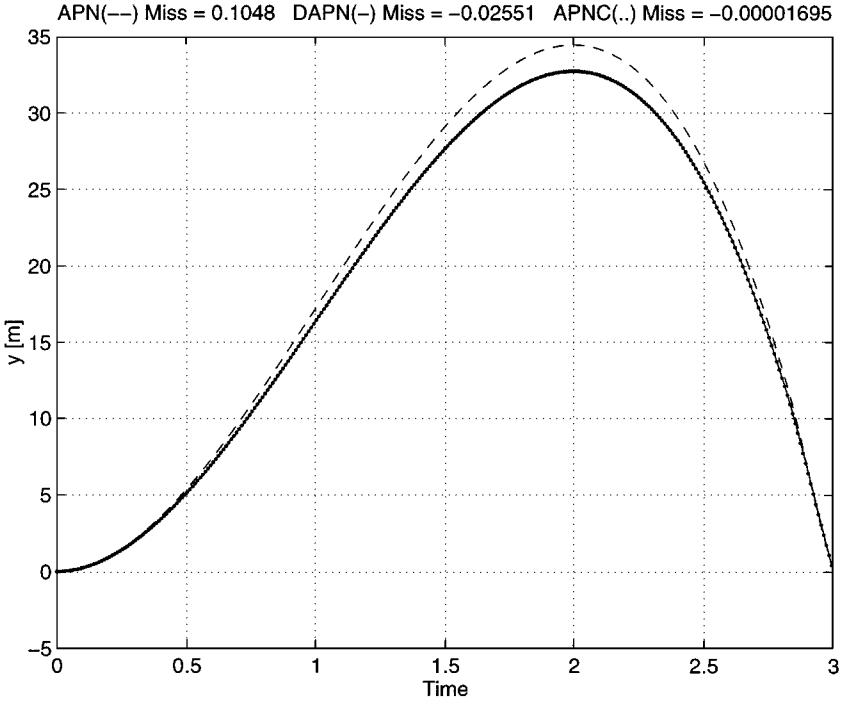

Fig. 1 Relative separation, in meters, for perfect intercept.

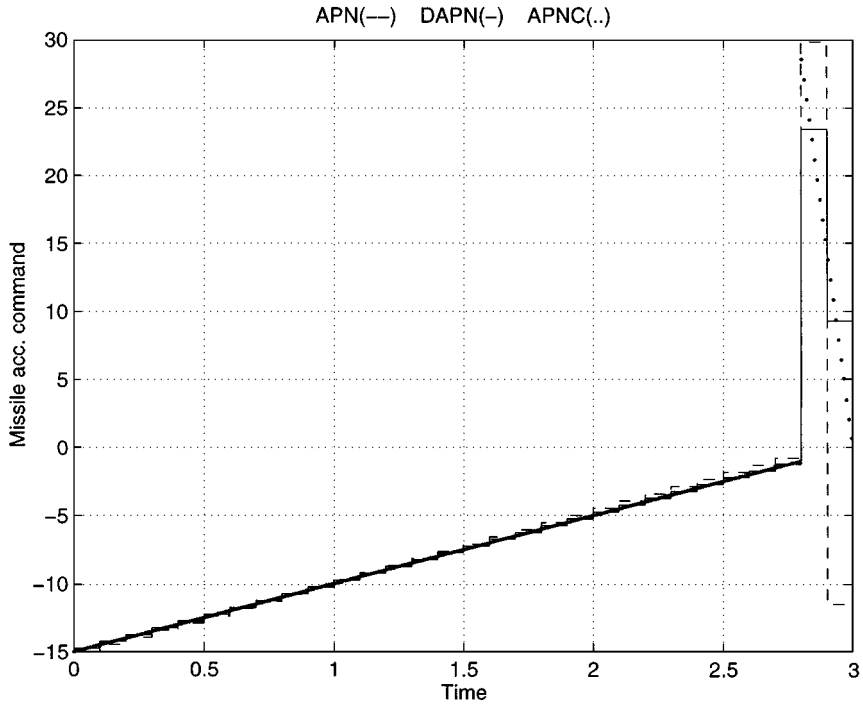

Fig. 2 Missile acceleration command for perfect intercept in *g*'s.

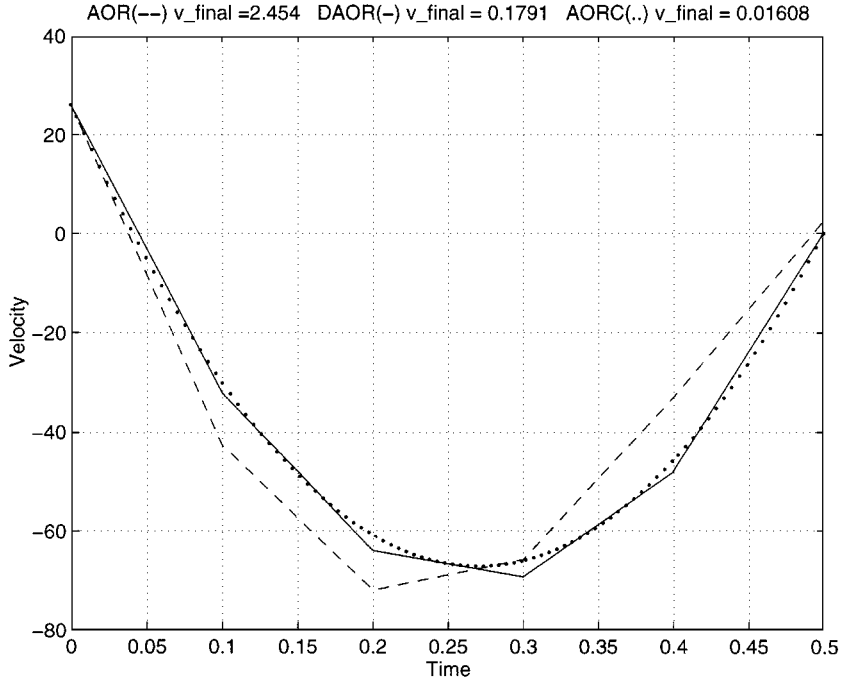

Fig. 3 Relative velocity, in meters per second, for perfect rendezvous.

For this example reducing h to 0.005 s narrows the differences between the competing guidance laws to an insignificant level.

V. Concluding Remarks

This Note has focused on discrete-time pursuit–evasion conflicts where both pursuer and evader models are without dynamics, i.e., unit transference, and where the evader maneuvers are exactly known. For such conflicts, our results include the discrete-time versions of the most popular guidance laws of PN, APN, and perfect rendezvous in closed-form formulas, enabling an easy realization with digital autopilots or remote guidance computers. A simulation study was performed to compare our discrete-time optimal guidance laws, with the guidance laws that emerge from just sampling the outputs of the classical continuous-time guidance laws. The results are promising and show a clear advantage of the discrete-time version of the classical guidance laws.

References

[1]Bryson, A. E., and Ho, Y. C., *Applied Optimal Control*, Hemisphere, New York, 1975, pp. 154, 155, 271–293.

[2]Zarchan, P., *Tactical and Strategic Missile Guidance*, AIAA, Washington, DC, 1990, pp. 153–156.

[3]Shefer, M., "Optimization of Closed-Loop Tactics in Ballistic Defense–Offense Scenarios," *Proceedings of the 32nd Israel Annual Conference on Aerospace Sciences*, Tel-Aviv, Israel, 1992, pp. 363–367.

[4]Ben-Asher, J. Z., "Linear-Quadratic Pursuit Evasion Games with Terminal Velocity Constraints," *Journal of Guidance, Control, and Dynamics*, Vol. 19, No. 2, 1996, pp. 499–501.

[5]Gitizadeh, R., Yaesh, I., and Ben-Asher, J. Z., "Discrete-Time Optimal Guidance," 38th Annual Israel Conference on Aerospace Sciences, Tel-Aviv, Israel, 1998, pp. 137–144.